

contain a trapped component of xenon which is from deep inside the earth, and that the higher xenon content of sample 2 is due to a component of atmospheric xenon in this sample. It seems likely that there was a larger degree of atmospheric contamination in sample 2 owing to the use of the auxiliary vacuum system for melting the sample and collecting the gases on charcoal.

The excess amounts of xenon at masses 128 and 129 are indicated as ^{128r}Xe and ^{129r}Xe , respectively, at the bottom of Table 1. The amounts of ^{128r}Xe and ^{129r}Xe were computed relative to the xenon from deep well gas for sample 1 and relative to the xenon in the atmosphere for sample 2. The concentration of ^{129r}Xe is the same in both samples in spite of the large variation in total xenon content. This ^{129r}Xe is attributed to the in situ decay of ^{129}I that was present with the more abundant ^{127}I isotope when the iodyrite formed. The concentration of ^{128r}Xe varies by about a factor of 2 in these two samples. This ^{128r}Xe is probably due to neutron capture on ^{127}I over the lifetime of the iodyrite.

A minimum value of the $^{129}\text{I}/^{127}\text{I}$ ratio that was incorporated into the ore can be obtained by assuming that all of the ^{129}I has since decayed to ^{129}Xe . This yields an $^{129}\text{I}/^{127}\text{I}$ ratio of $\cong 2.2 \times 10^{-15}$ for sample 1 and of $\cong 2.4 \times 10^{-15}$ for sample 2.

To estimate an upper limit for the $^{129}\text{I}/^{127}\text{I}$ ratio that was incorporated into the iodyrite, it is necessary to estimate a minimum age for the iodyrite. An approximate value for the minimum age of the iodyrite can be obtained from the amount of ^{128r}Xe in the ore if the neutron flux rate can be estimated during the lifetime of the ore. If the iodyrite was exposed to the typical neutron flux reported for granitic rocks, ≈ 10 neutron $\text{cm}^{-2} \text{yr}^{-1}$ (13), then the excess ^{128r}Xe and the thermal neutron cross section of ^{127}I (≈ 6.2 barns) can be used to estimate the age of the iodyrite samples. This calculation yields an age of 67.7×10^6 years for sample 1 and an age of 30.5×10^6 years for sample 2, in good agreement with the age limits estimated for iodyrite (10). These ages yield maximum values of the $^{129}\text{I}/^{127}\text{I}$ ratio incorporated in the ore: $^{129}\text{I}/^{127}\text{I} \leq 2.3 \times 10^{-15}$ for sample 1 and $^{129}\text{I}/^{127}\text{I} \leq 3.3 \times 10^{-15}$ for sample 2.

Thus it is estimated that the iodyrite samples formed from iodine with an isotopic composition of $3.3 \times 10^{-15} \cong$

$^{129}\text{I}/^{127}\text{I} \cong 2.2 \times 10^{-15}$. Since the value calculated for the maximum $^{129}\text{I}/^{127}\text{I}$ ratio depends critically on the neutron flux assumed, it should be noted that a higher neutron flux would increase our estimate of the maximum $^{129}\text{I}/^{127}\text{I}$ ratio. However, gas loss over geologic time would reduce the content of both ^{129r}Xe and ^{128r}Xe , and this process would cause minimum errors in the limit calculated for the maximum $^{129}\text{I}/^{127}\text{I}$ ratio.

B. SRINIVASAN
E. C. ALEXANDER, JR.*
O. K. MANUEL

Department of Chemistry, University
of Missouri, Rolla 65401

References and Notes

1. J. H. Reynolds, *Phys. Rev. Lett.* **4**, 8 (1960).
2. P. M. Jeffery and J. H. Reynolds, *J. Geophys. Res.* **66**, 3582 (1961); P. K. Kuroda and O. K. Manuel, *ibid.* **67**, 4859 (1962); C. M. Hohenberg, F. A. Podosek, J. H. Reynolds,

- Science* **156**, 233 (1967); D. D. Sabu and P. K. Kuroda, *Nature* **216**, 442 (1967).
 3. E. C. Alexander, Jr., and O. K. Manuel, *Earth Planet. Sci. Lett.* **4**, 113 (1968).
 4. O. K. Manuel, E. C. Alexander, Jr., D. V. Roach, R. Ganapathy, *Icarus* **9**, 291 (1968).
 5. B. C. Purkayastha and G. R. Martin, *J. Inorg. Nucl. Chem.* **24**, 755 (1962).
 6. R. R. Edwards, *Science* **137**, 851 (1962).
 7. E. C. Alexander, Jr., B. Srinivasan, O. K. Manuel, *Earth Planet. Sci. Lett.* **5**, 478 (1969).
 8. T. P. Kohman and R. R. Edwards, *U.S. AEC Rep. NYO-3624-1* (1966).
 9. J. R. Richards and R. T. Pidgeon, *J. Geol. Soc. Aust.* **10**, 243 (1963).
 10. L. J. Lawrence, personal communication.
 11. G. A. Bennett and O. K. Manuel, *Geochim. Cosmochim. Acta* **34**, 593 (1970).
 12. A. O. Nier, *Phys. Rev.* **79**, 450 (1950).
 13. P. Morrison and J. Pine, *Ann. N.Y. Acad. Sci.* **62**, 69 (1955).
 14. Investigation supported by NSF grant GA-16618. The samples were purchased from the Southwest Scientific Company. We are grateful to the following for advice on the geology of Broken Hill iodyrites: Dr. L. J. Lawrence of the University of New South Wales; Dr. B. W. Hawkins of C. R. A. Exploration Party, Limited, Melbourne, Australia; and Dr. R. O. Chalmers of the Australian Museum, Sydney.
- * Present address: Department of Physics, University of California, Berkeley 94720.
- 16 February 1971; revised 29 April 1971

Microearthquakes in the Ahuachapan Geothermal Field, El Salvador, Central America

Abstract. Microearthquakes occur on a steeply dipping plane interpreted here as the fault that allows hot water to circulate to the surface in the geothermal region. These small earthquakes are common in many geothermal areas and may occur because of the physical or chemical effects of fluids and fluid pressure.

The study of microearthquakes provides a way of mapping active faults in regions with few large earthquakes (1, 2). The microearthquakes discussed here, with magnitudes as small as 0 (3, 4), can best be recorded by ultra-sensitive, high-frequency seismographs operated at hypocentral distances of less than a few tens of kilometers. More than 10,000 microearthquakes may occur in a region where only one earthquake has been located during the same period by the U.S. Coast and Geodetic Survey (now the National Ocean Survey) with teleseismic data. Thus, microearthquake data sufficient to outline faults can often be collected in a few days, weeks, or months.

Microearthquakes are observed in many major geothermal areas studied in Iceland, California, and Japan (3-6). The epicenters typically occur within the region of geothermal alteration of the surface rocks and the foci are often between 1 and 10 km deep. Earthquakes usually occur on faults, and, in many geothermal areas, faults provide the main channel along which hot water reaches either the surface or a highly permeable horizon near the surface (7).

Recent data suggest that fluids present along faults play a significant role in determining where, when, and in what time sequence tectonic stress is relieved as seismic energy (4, 8). Two effects of fluids may be important: pore pressure (9) and stress corrosion (10). High pore pressure reduces the frictional resistance to fracture. High stresses at crack tips increase the chemical reaction of the rock with the pore fluid and thus enhance fracturing. These effects may also lead to an increase in microearthquake activity when geothermal brines are reinjected for disposal purposes.

Three vertical-component seismometers were operated 2 to 3 km apart in the Ahuachapan geothermal area in El Salvador from 7 December 1969 to 10 August 1970 (Fig. 1). Two horizontal-component seismometers were also placed at site A. The system response had maximum gain of about 500,000 at 17 cycle/sec. All seismic signals and a time signal were connected by cable to a magnetic tape recorder situated at point A. About 500 earthquakes were recorded and analyzed during the total of 6 months that the equipment at site

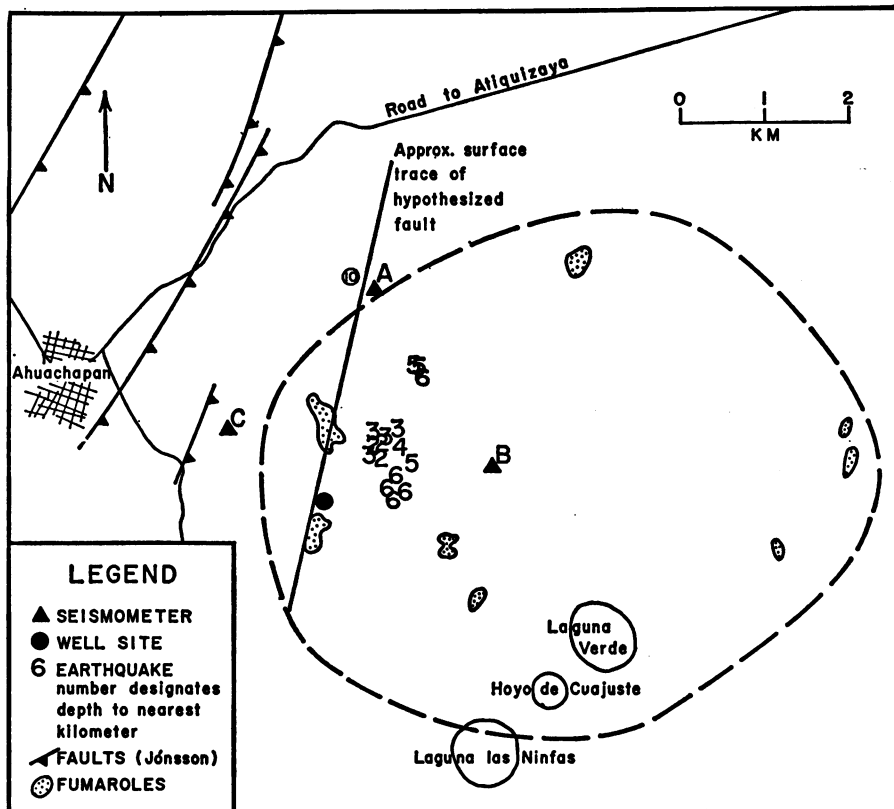


Fig. 1. Map of the Ahuachapan geothermal area. The center of this map is located at approximately $13^{\circ}55'N$ and $89^{\circ}50'W$. Dashed line shows limits of caldera as mapped by Jónsson (13); A, B, and C are seismometer sites.

A worked properly. The distribution of S-wave minus P-wave arrival times is shown in Fig. 2. The S-P time multiplied by a velocity of 8 km/sec is approximately equal to the hypocentral distance. Two groups of events can be distinguished. Over 150 events with S-P times of less than 8 seconds occur near the geothermal region. About 350 events with S-P times greater than 8 seconds most likely occur on the seismic zone that dips northeastward under El Salvador from the Middle American Trench (11). The magnitudes of the more distant events are generally 2.5 to 3 units higher than the magnitudes of the local events. The U.S. Coast and Geodetic Survey reports hypocenters of 32 events between 1961 and 1970 with magnitudes greater than 3.5 located within 60 km epicentral distance of Ahuachapan at depths of 16 to 276 km. These large events lie along or above the dipping seismic zone and do not appear to be directly related to the surficial geothermal activity.

An average of one microearthquake per day occurred in the geothermal area. When corrected for different instrument gains, this average activity is roughly 5 to 15 times less than the activity recorded in the Krisuvik and Hen-

gill geothermal areas in Iceland (3, 4). The local events tended to occur in swarms of 10 to 20 events spaced days and weeks apart. Such swarm type sequences were also noted in geothermal areas in Iceland (4). Only 17 of these local earthquakes could be located accurately because of difficulties in keep-

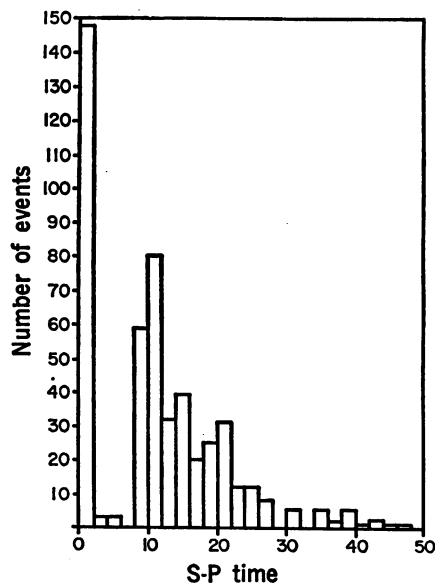


Fig. 2. Distribution of S-P times for earthquakes recorded at Ahuachapan.

ing the long signal cables operative. The epicenters of these events are shown in Fig. 1, and in Fig. 3 the hypocenters are projected onto a vertical plane striking $N80^{\circ}W$ through the geothermal region, perpendicular to the epicentral trend of earthquakes at similar depths shown in Fig. 1. The hypocenters in Fig. 3 are represented by rectangles that show the approximate error in location determined by reading several times all reasonable choices for P- and S-wave arrival times. A constant P-wave velocity of 4 km/sec and S-wave velocity of 2.2 km/sec are assumed, based on experience in other geothermal areas (4, 5, 12). Any reasonable change in the assumed velocity changes the strike and dip of the seismic plane slightly but does not move the hypocenters from a plane.

The fault plane in Fig. 3 is chosen to intersect as many of the hypocenters as possible and to pass through the point where fault breccia is observed in the drill hole (13) shown in Figs. 1 and 3. Reliable fault-plane solutions are not possible because of the few stations and uncertainties in instrument polarity after cable failures. This plane is approximately parallel to normal faults mapped to the northwest (13) (Fig. 1). The existence of faults in the geothermal region was suggested but has not been definitely proved from geologic data (13). The regions of fumarole activity could each lie on one of three faults trending nearly parallel to the plane of seismic activity. Data were not collected in sufficient quantity to determine if there is seismic activity in the eastern part of the geothermal field. An alternative hypothesis is that the occurrence of fumaroles and the fault breccia in the well can be explained by the presence of a caldera now obscure because of erosion (13).

Geothermal ground noise has been noted in several geothermal areas (14). A three-component seismic system with frequency response peaked between 10 and 350 cycle/sec was operated near fumaroles and wells, and along profiles traversing the western part of the geothermal field in December 1969. No systematic variation in the frequency or energy of the ground noise was observed except that the power of the high-frequency noise (10 to 50 cycle/sec) generated by blowing geothermal wells, rivers, and fumaroles is attenuated at a rate of about 3 db per 50 m of distance in this area.

Data from this study strongly suggest the existence of a seismically active

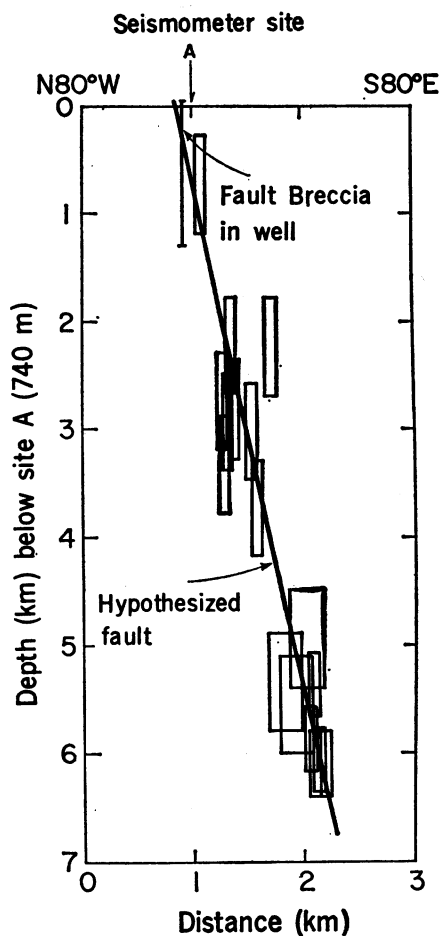


Fig. 3. Cross section through the geothermal area. Hypocenters of earthquakes are shown by rectangles. The vertical line just left of seismometer site A represents the well shown in Fig. 1.

fault directly under the best producing wells in the Ahuachapan geothermal area. Production wells in the future might best be drilled to intercept this fault. Such simple microearthquake studies provide a powerful method of mapping active faults and can, therefore, be of considerable practical and economic importance in the location and utilization of geothermal heat sources.

PETER L. WARD
KLAUS H. JACOB

Lamont-Doherty Geological
Observatory of Columbia University,
Palisades, New York 10964

References and Notes

1. See, for example, J. Oliver, A. Ryall, J. N. Brune, D. B. Slemmons, *Bull. Seismol. Soc. Am.* **56**, 899 (1966); L. Seeber, M. Barazangi, A. Nowroozi, *ibid.* **60**, 1669 (1970).
2. J. N. Brune and C. R. Allen, *ibid.* **57**, 277 (1967).
3. P. L. Ward, G. Palmason, C. Drake, *J. Geophys. Res.* **74**, 664 (1969).
4. P. L. Ward and S. Björnsson, *ibid.* **76**, 3953 (1971).
5. For California: A. L. Lange and W. H. Westphal, *ibid.* **74**, 4377 (1969).
6. For Japan: I. Kasuga, *J. Geogr. Tokyo* **76**, 76 (1967).
7. J. W. Elder, in *Terrestrial Heat Flow*, W. H. K. Lee, Ed. (American Geophysical Union,

- Monogr. 8, Washington, D.C., 1965), p. 211; J. R. McKnit, *ibid.*, p. 240; G. W. Grindley, *Bull. N.Z. Geol. Surv.* **75**, 131 (1965).
8. D. M. Evans, *Geotimes* **10**, 11 (1966); J. H. Healy, W. W. Rubey, D. T. Griggs, C. B. Raleigh, *Science* **161**, 1301 (1968); C. B. Raleigh, J. Bohn, J. H. Healy, *Trans. Am. Geophys. Union* **51**, 351 (1970).
9. M. K. Hubbard and W. W. Rubey, *Bull. Geol. Soc. Am.* **70**, 115 (1959).
10. C. H. Scholz, *J. Geophys. Res.* **73**, 3295 (1968).
11. P. Molnar and L. R. Sykes, *Bull. Geol. Soc. Am.* **80**, 1639 (1969).
12. G. Palmason, *Soc. Sci. Islandica*, No. 40 (1971).
13. J. Jónsson, "Report to United Nations DP Survey of Geothermal Resources in El Salva-

- dor" (United Nations Resources and Transport Division, Energy Section, New York, 1970).
14. P. C. Whiteford, *United Nations Symposium* (Pisa, Italy, 1970), in press; G. R. T. Clacy, *J. Geophys. Res.* **73**, 5377 (1968).
15. Contribution No. 1674 from Lamont-Doherty Geological Observatory of Columbia University of Columbia University. This work was supported by United Nations purchase order 9-20-11471. Special thanks to the staff of the U.N. Resources and Transport Division in El Salvador and the Comision Ejecutiva Hidro-electrica del Rio Lempa, who assisted in the fieldwork. Drs. Bryan Isacks and Jack Oliver critically reviewed the manuscript.

29 March 1971

Cerebrospinal Fluid Production by the Choroid

Plexus and Brain

Abstract. The production of cerebrospinal fluid and the transport of ^{24}Na from the blood to the cerebrospinal fluid were studied simultaneously in normal and choroid plexectomized rhesus monkeys. Choroid plexectomy reduced the production of cerebrospinal fluid by an average of 33 to 40 percent and the rate of appearance of ^{24}Na in the cerebrospinal fluid and its final concentration were proportionately reduced. In both normal and plexectomized animals, ^{24}Na levels were found to be markedly greater in the gray matter surrounding the ventricles and in the gray matter bordering the subarachnoid space. That sodium exchanges in these two general areas of the brain may be linked to the formation of the cerebrospinal fluid is discussed here.

Although numerous studies (1-3), including the classical experiments of Dandy and Blackfan (4, 5), have pointed to the choroid plexuses as the exclusive site of cerebrospinal fluid (CSF) secretion, this view has not gone unquestioned (6-8). Evidence has been advanced, for example, that at least a limited amount of CSF can be formed extrachoroidally in the cerebral ventricles (6), the aqueduct of Sylvius (7), and the subarachnoid space (8). In a recent study, the production of CSF after choroid plexectomy was estimated to be far more substantial than previously reported (9). On the basis of studies on 76 choroid plexectomized rhesus monkeys, these conclusions were reached: (i) The production of CSF rostral to the fourth ventricle (determined by ventriculo-aqueductal perfusion of the CSF with [^{14}C]-inulin) was reduced by only one-third after choroid plexectomy; (ii) the composition of the CSF after choroid plexectomy was unchanged; and (iii) the surgical obstruction of the choroid plexectomized ventricles resulted in acute and progressive hydrocephalus that was only slightly less severe than that occurring in nonplexectomized ventricles with similar obstructions (9).

In this study, we have compared the production of CSF and the transport of ^{24}Na from the blood to the CSF in normal and choroid plexectomized rhesus

monkeys. The animals ranged in age between 1½ to 2 years and varied in weight between 2 and 3 kg. In six animals, the choroid plexuses of both lateral ventricles had been removed 3 to 9 months before the current experiments [the technique of choroid plexectomy and the histological consequences of the procedure have been reported elsewhere (9)]. Eleven animals served as normal, nonplexectomized controls. In all animals, the fourth ventricle was obstructed with an inflatable balloon at the beginning of each experiment (Fig. 1). A lateral ventricle-to-lateral ventricle perfusion was then arranged, in which a Harvard pump apparatus with an inflow rate of 0.191 ml/min was used. The ventricular perfusate consisted of artificial CSF to which the following tracers were added: (i) ^{14}C -labeled inulin (20 μC per 30 ml of perfusate); (ii) dextran 2000 (15 mg per 30 ml of perfusate), and (iii) ^3H -labeled sucrose (15 μC per 30 ml of perfusate). Simultaneously, an intravenous infusion of ^{24}Na (0.4 mc per experiment) was administered so as to establish a steady-state level of the isotope in the blood (± 3 to 8 percent variation from mean counts per minute per microliter). During each experiment, serial samples of plasma and outflow perfusate were taken at 15-minute intervals. Inflow samples were obtained at the beginning and end of each perfusion period, and